Chapter 6

Applications of the Fuzzy Logic to the Energy Conversion Systems on Board of UAVs

Dinca Liviu and Corcau Jenica Ileana

Additional information is available at the end of the chapter

http://dx.doi.org/10.5772/67992

Abstract

This chapter intends to present some applications of the fuzzy controllers to the automatic control of the DC-to-DC converters type boost, buck and buck-boost. For the mathematical modelling of these converters, one used averaged models; taking into account that controlled parameter is the average output voltage. One considered only the continuous conduction mode in the mathematical model. For each converter, one makes a short description of the principal scheme and the functioning mode and presents the averaged model. One obtains the transfer functions and finally builds fuzzy controllers in order to stabilize the output voltage with respect to the input voltage variations. The control is realized by modifying the duty cycle of the PWM command pulses. Obtained systems, both in closed loop and in open loop, are implemented in MATLAB/Simulink and simulations results are also presented.

Keywords: DC-to-DC converters, fuzzy logic control, averaged models, UAV, power systems

1. Introduction

Type UAV (Unmanned Air Vehicle) platforms have realised in the last period a special development due to their large area of applicability. UAVs can perform a variety of missions like military observation, combat, crops observations, disaster areas surveillance, in conditions of very high econommic and energy efficiency against classical aviation. UAVs offers many advantages like reduced manufacturing and operating costs, low energy consumption, possibility to access safely in hazardous areas for manned aircrafts, ability to penetrate spaces more restricted, inaccessible to classic aircraft, and due to technological developments obtained recently, the ability to achieve continuous flight missions with durations of the order of several days to several weeks. In this sense, the development of UAVs is expected to play an important role in High Altitude Pseudo-Satellites (HAPS) with continuous flight duration of the order of 5 years.

Achieving such high flight duration was possible due to the use of hybrid power sources that use at least two types of energy sources. In this sense, the most used energy sources are presently high capacity batteries or super capacitors that are recharged from renewable energy sources, especially high-efficiency photovoltaic cells developed in the last period. Fuel cells present a high efficiency, so it represents an alternative for the electrically powered manned airplanes. This solution is extensively studied and planned to be used in the near future. Airbus Company has already developed an electric airplane for two flights that last approximately for 1 hour. Currently, it is working to develop a plane for four persons with hybrid power source (high capacity battery plus two-stroke combustion engine that acts as an electric generator). Flight duration is expected to be extended to two hours. Research department of Airbus is considering replacing the thermal engine with the fuel cell to further expand the duration of flight.

Titan Aerospace was tested in August 2013, a concept vehicle for future high-altitude SOLAR 50 and 60 UAVs. SUN SOLAR 50 was scheduled to fly in 2014. SOLAR 50 was conceived as a UAV which uses high-capacity batteries and 3000 solar cells as power sources. The maximum flight duration of 50 SOLAR is expected to be 5 years at last. It is designed to be equipped with telecommunications and recognition systems, atmospheric sensors, etc. SUN 60 is planned for a payload of 125 kg [1–3].

The High Altitude Long Endurance Boeing (HALE) UAS 2012 aims at developing high altitude UAS for missions to ensure transmissions for the disposal of existing infrastructure and prolonged surveillance missions to the areas of interest.

Phantom Eye Project uses hydrogen internal combustion engine with hydrogen stored cryogenically. Solar Eagle Project, of Boeing as well, expects the use of high efficiency solar cells and SOFC type fuel cells. Wingspan aircraft is expected to be 120 m and propulsion will use six electric motors with permanent magnets [1–3].

Project Zephyr 7 High Altitude Pseudo-satellites from Airbus Defence & Space is to be used for surveillance, communications and monitoring services on surfaces in the order of tens of thousands km^2. This UAV holds the record for the longest flight—336 hours. Solar energy has been used for the propulsion and storage in lithium-ion battery with 3 kWh capacities to drive at night [1–3].

Since the parameters of power sources such as solar cells or fuel cells vary greatly in relation to the operating conditions, and loads useful on board UAVs (cameras, sensors, communications systems, etc.) usually require stabilized voltage, power buses of UAVs need to be maintained at a constant voltage.

This can be achieved by using power converters to adapt output sources to the requirements of bus power sources. Most sources on board UAVs are DC sources and loads are mostly (except some propulsion motors) of DC types. Following are required DC-to-DC converter types which have a higher efficiency and weight as low as possible aboard UAVs. The most convenient in this sense are the converters that have not transformed, part of this class are buck, boost and buck-boost converters. They are suitable for use on UAVs because they adapt the power source voltage to the power bus voltage by simply varying the duty cycle of the command pulses.

http://dx.doi.org/10.5772/67992

For the converters control, there are many techniques in literature, more or less sophisticated, among these are fuzzy techniques. These techniques offer a robust control and have an advantage which is related to human logic that these techniques do not require to know a detailed mathematical model of the system and can be tuned relatively easily granted by numerical simulations.

In this chapter, development of models used in the study of electrical systems of UAVs follows the modelling of three types of DC-DC converters, used on board UAVs, and development of fuzzy controllers is used to stabilize the output voltage.

Mathematical models developed for these converters follow the behaviour in terms of the averaged parameters (voltage and current) and neglect their ripples.

Although all models are being averaged, technique for obtaining these models is the introduction of the circuit voltage or current sources to make up in terms of DC parameters switch, coil or diodes present in converters. We consider this method more viable in terms of logic than writing equations split by two periods of operation of the converter and then their average as shown in Ref. [4].

2. Boost converter

The principal scheme of the boost converter is shown in **Figure 1a** and **b** equivalent scheme for continuous mode is presented. Functioning of this converter contains two steps. In the first step when the switch is in position 1, the inductor current rises and the inductor accumulate energy in its electromagnetic field. In the second step when the switch is in position 2, the inductor is now in series with the input source and pushes its energy on the capacitor. Inductor current drops, so the inductor behaves as voltage source in series with the input source and the capacitor will be charged to a voltage higher than the input voltage. For this reason, the boost converter raises the input voltage [5, 6].

Diagram in **Figure 1a** is equivalent in terms of DC components with the diagram in **Figure 1b**. Given that, coil behaviour was modelled in terms of averaged voltage with a voltage source dependent on the duty cycle of the control pulses $U_L(d)$, and the current through the switch was modelled by a current source dependent on the duty cycle of control pulses $I_T(d)$.

Coil voltage was found to be $U_L = \frac{d \cdot U_{\text{in}}}{1-d}$ so as to respect the converter transfer characteristic in steady state. Regarding the currents, it was considered that $I_T = I_D$ in terms of the average

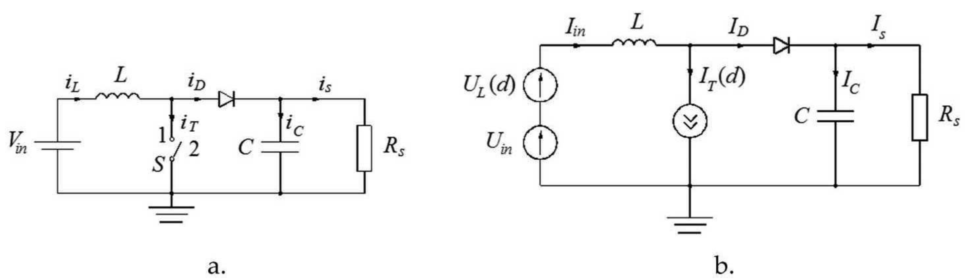

Figure 1. Boost converter. (a) Principal scheme, (b) Equivalent scheme for continuous mode.

values. In stationary regime, coil L behaves like a voltage source $U_L(d)$. At a duty cycle variation, in transitory regime. In these conditions, one can write relations:

$$\begin{cases} \dfrac{dI_{\text{in}}}{dt} = -\dfrac{1}{L}U_C + \dfrac{U_{\text{in}}}{L(1-d)} \\ \dfrac{dU_C}{dt} = \dfrac{1}{2C}I_{\text{in}} - \dfrac{U_C}{CR_S} \end{cases} \tag{1}$$

For linearization, notations, $I_{\text{in}} = I_{\text{in}0} + \Delta I_{\text{in}}$, $U_C = U_{C0} + \Delta U_C$, $U_{\text{in}} = U_{\text{in}0} + \Delta U_{\text{in}}$, $d = d_0 + \Delta d$ have been used. Relation obtained after linearization is (2)

$$\begin{cases} \begin{bmatrix} \Delta I_{\text{in}} \\ \Delta U_C \end{bmatrix} = \begin{bmatrix} 0 & -\dfrac{1}{L} \\ \dfrac{1}{2C} & -\dfrac{1}{CR_S} \end{bmatrix} \begin{bmatrix} \Delta I_{\text{in}} \\ \Delta U_C \end{bmatrix} + \begin{bmatrix} \dfrac{1}{L(1-d)} & \dfrac{U_{\text{in}}}{L(1-d)^2} \\ 0 & 0 \end{bmatrix} \begin{bmatrix} \Delta U_{\text{in}} \\ \Delta d \end{bmatrix} \\ [\Delta U_{\text{out}}] = [0 \quad 1] \begin{bmatrix} \Delta I_{\text{in}} \\ \Delta U_C \end{bmatrix} + [0 \quad 0] \begin{bmatrix} \Delta I_{\text{in}} \\ \Delta d \end{bmatrix} \end{cases} \tag{2}$$

Using this system, one can deduce the transfer functions given in Eqs. (3) and (4)

$$H_1(s) = \frac{\Delta U_{\text{out}}(s)}{\Delta U_{\text{in}}(s)} = \frac{\frac{1}{2LC(1-d)}}{s^2 + s\frac{1}{CR_S} + \frac{1}{2LC}} = \frac{k_1}{(s-s_1)(s-s_2)} \tag{3}$$

$$H_2(s) = \frac{\Delta U_{\text{out}}(s)}{\Delta d(s)} = \frac{\frac{U_{\text{in}}}{2LC(1-d)^2}}{s^2 + s\frac{1}{CR_S} + \frac{1}{2LC}} = \frac{k_2}{(s-s_1)(s-s_2)} \tag{4}$$

In **Figure 2**, simulation scheme of boost converter in open loop is shown. They were used ΔU_{in} and Δd as input, the output voltage was considered as ΔU_{out}. Simulated boost converter parameters were as follows $L = 47\ \mu\text{F}$, $C = 2.2\ \text{mF}$, $R_S = 1\ \Omega$, $d = 0.5$, $U_{\text{in}} = 24\ \text{V}$. In the simulations using transfer functions, variations of output voltage about output voltage reference,

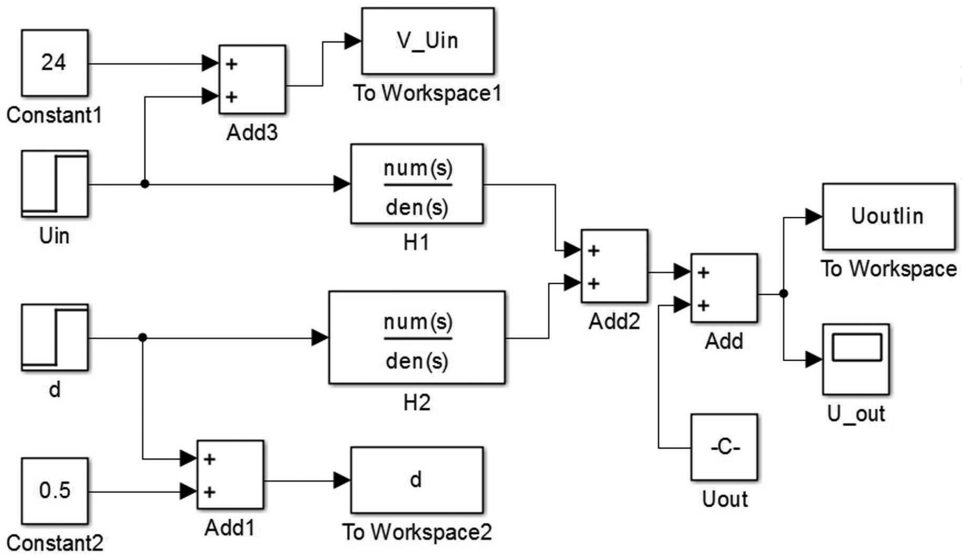

Figure 2. Open loop simulation scheme of boost converter.

when there are some variations in input voltage and duty cycle compared to reference values, are obtained. To capture the absolute values, some sum blocks are introduced in **Figure 2** whose variations overlap reference values achieved through the transfer or the absolute values of the input parameters. Simulation results are presented in **Figure 3a–c**.

Fuzzy control technique for DC-DC converters is applied in some studies in literature [7–10]. Other control techniques for these converters are studied in Refs. [11–17].

Closed loop scheme of the boost converter, implemented in MATLAB/Simulink is shown in **Figure 4**. One used a fuzzy controller with two inputs, output voltage error with respect to the

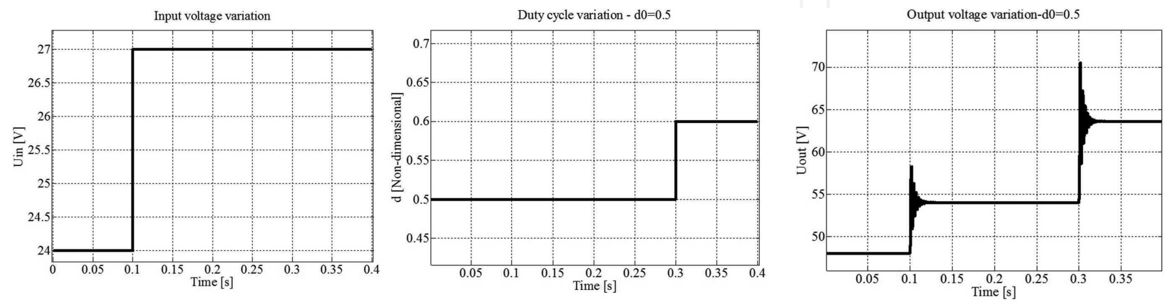

a. b. c.

Figure 3. Boost converter response: (a) input voltage variation; (b) duty cycle variation; (c) output voltage variation.

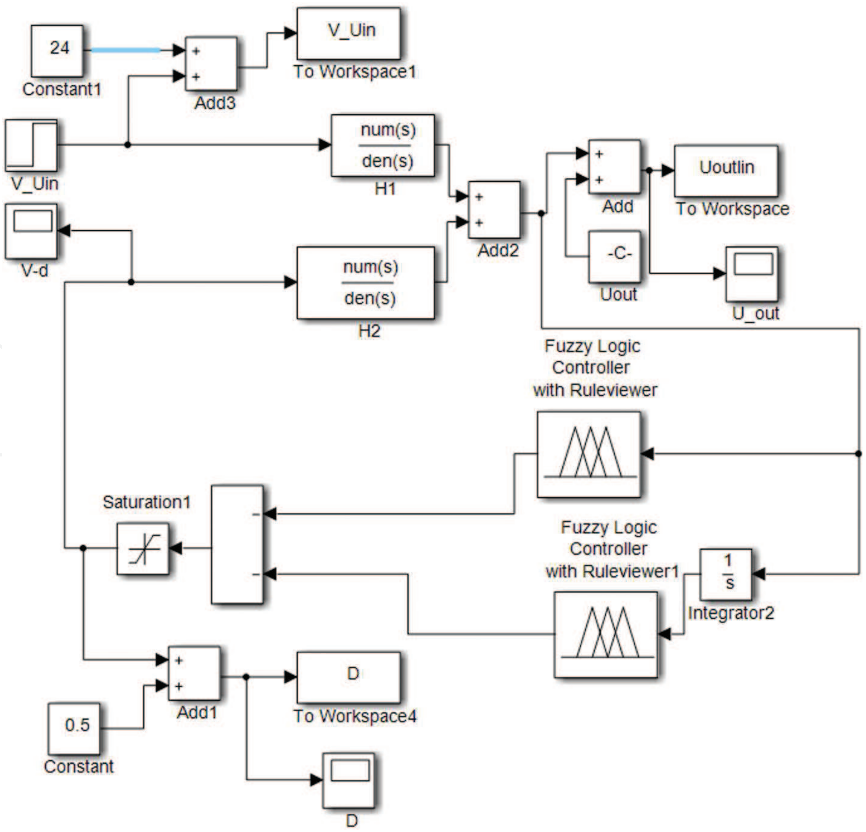

Figure 4. Closed loop simulation scheme for boost converter.

nominal output voltage and its integral, so one can say that this is a PI fuzzy controller. The advantage of the fuzzy controllers is that one can modify conveniently the control characteristics slopes in order to obtain the desired system behaviour. Usually one wishes a higher slope for points far from the origin and smaller slope for points near the origin. In this way, when the system is far from the nominal functioning point, one can accelerate its return to the nominal point. When it comes near the nominal point, parameters variations are sluggish in order to obtain a good stability in the nominal point. Fuzzy system in **Figure 4** has a particularity for an error and its integral are defined by two separate fuzzy controllers with four membership functions on input and output. In this way, one can simplify the controller tuning. There are necessarily eight inference rules (four rules for each controller) in contrast with the classical fuzzy controller with two inputs and one output having 16 inference rules. This difference increases once the membership function for each input increases. In **Figure 5**, the membership functions for fuzzy proportional controller P and its control surface are presented.

In **Figure 6**, the membership functions for fuzzy integrator controller I and its control surface are presented. Converter operation with these fuzzy controllers has been tested to a step type signal and ramp type signal. In hybrid power systems of UAVs containing fuel cell or solar cells, parameters variations are not very sudden, so it is exciting to study the converters behaviour at sluggish signals, such as the ramp type which is taken into consideration here. In **Figure 7**, the boost converter behaviour at step signal is shown and in **Figure 8**, its behaviour to a ramp signal with a slope of 3 V/s is shown.

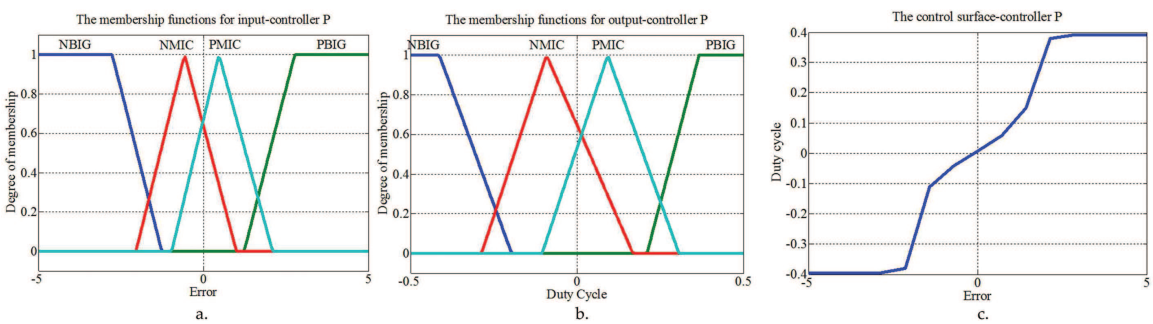

Figure 5. P-fuzzy controller. (a) Input membership functions; (b) Output membership functions; (c) Control surface.

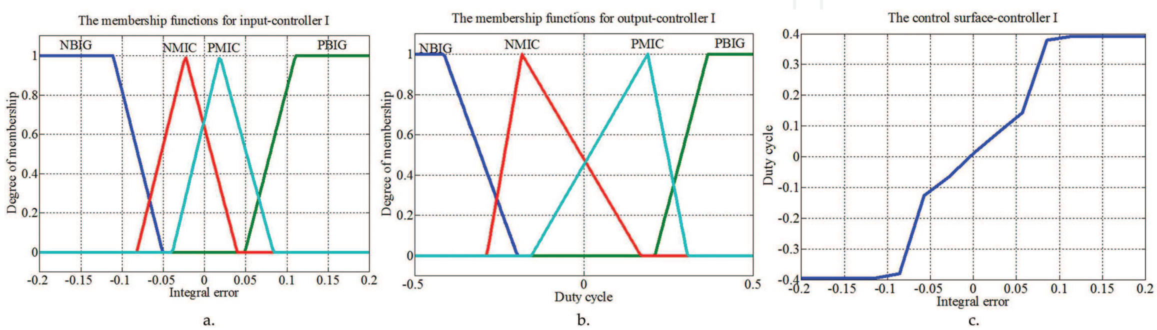

Figure 6. I-fuzzy controller. (a) Input membership functions; (b) Output membership functions; (c). Control surface.

Linguistic terms for both the controllers and for both inputs and outputs are NBIG (large negative), NMC (small negative), PMC (small positive) and PBIG (big positive). For both controllers, inference rules are: If input is NBIG, then output is NBIG; If input is NMC, then output is NMC; If input is PMC, then output is PMC; If input is PBIG, then output is PBIG.

For defining the controllers in this case, it is intended to simplify them as much so as to reduce the computation time required. In this purpose, one eliminated the membership function corresponding to linquistic term ZERO, which is used in the usual manner in fuzzy controllers. By conveniently change of the membership function one obtained control surfaces in concordance with the followed strategy - lower slope around the origin and greater slope farther origin.

The behaviour of the converter closed loop is one adequate operation of power systems on UAVs. Peak voltages at step input are attenuated and voltage returns quickly enough to the prescribed value. For the ramp input, deviation from set point is only 0.025 V, which is a very good performance.

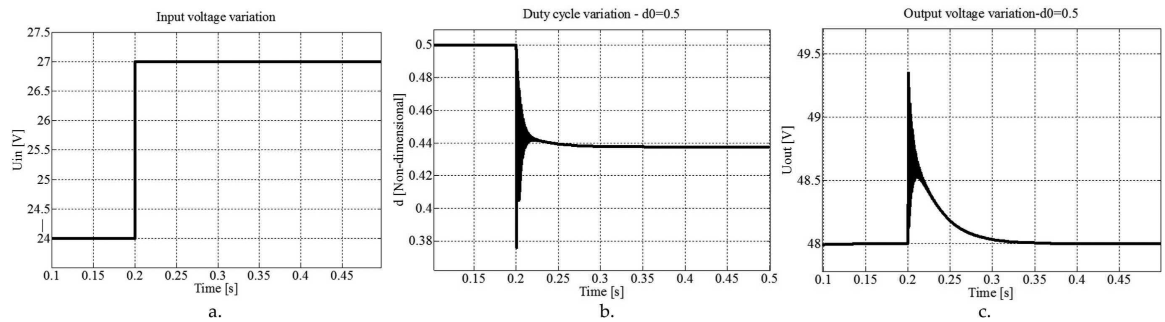

Figure 7. Closed loop behaviour of boost converter: (a) input variation; (b) duty cycle variation; (c) output voltage variation.

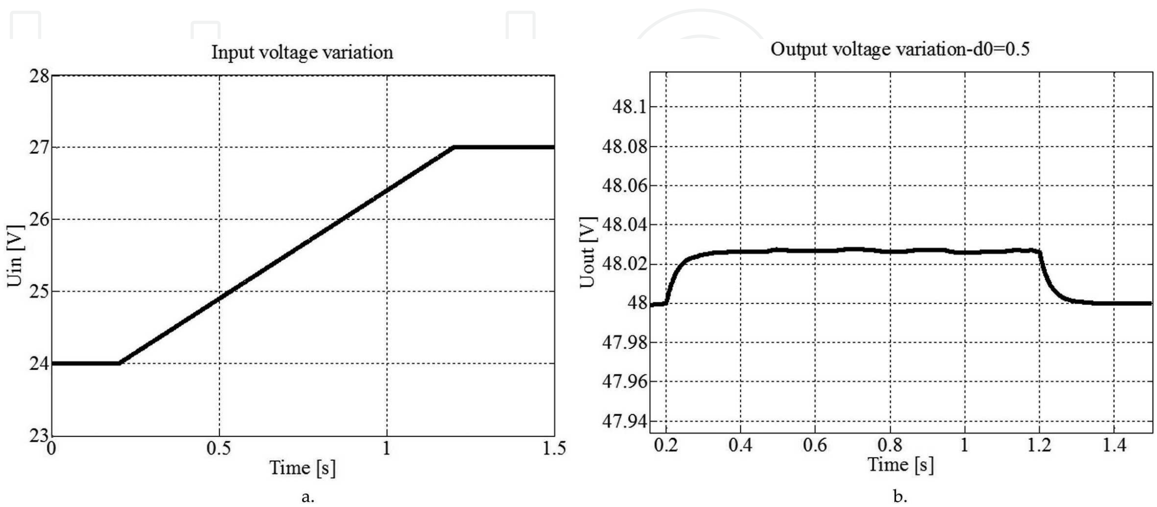

Figure 8. Boost converter behaviour at ramp signal: (a) input voltage variation; (b) output voltage variation.

3. Buck converter

Principal scheme of the buck converter is shown in **Figure 9**. This converter has also two steps in its functioning. In the second step when the switch is in position 1, the capacitor loads through the inductor and inductor current increases, so the inductor behaves as a voltage source with inverse polarity with respect to the input voltage. In this manner on the capacitor, one can obtain a voltage smaller than the input voltage. In the second step when the switch is in position 2, energy accumulated in the inductor is pushed on the capacitor and thus Inductor current decreases, so it behaves as a voltage source with the same polarity as the input voltage but with a smaller value. So, the buck converter decreases the input voltage. In **Figure 10**, equivalent scheme for continuous mode is presented.

Following **Figure 10**, one can write the following relations: $U_{\text{in}} - U_L = U_{\text{out}} = d{\cdot}U_{\text{in}},\ i_T + i_D = i_L = i_S,\ U_{in}{\cdot}i_T = U_{out}{\cdot}i_S$. After several transformations, following system of equations give:

$$\begin{cases} U_{\text{out}} = U_{\text{in}} d - L\dfrac{d}{dt}\left(\dfrac{I_T}{d}\right) \\ \dfrac{U_{\text{out}}}{R_S} = I_T\dfrac{1}{d} - C\dfrac{dU_{\text{out}}}{dt} \end{cases} \tag{5}$$

By linearization, like the case of the boost converter, resulted linearized model is:

$$\begin{cases} \Delta \dot{I_T} = -\dfrac{d_0}{L}\Delta U_{\text{out}} + \dfrac{d_0^2}{L}\Delta U_{\text{in}} + \dfrac{V_{\text{in}0}\cdot d_0}{L}\Delta d + \dfrac{I_{T0}}{d_0}\Delta \dot{d} \\ \Delta \dot{U}_{\text{out}} = \dfrac{1}{C\cdot d_0}\Delta I_T - \dfrac{1}{R_S\cdot C}\Delta U_{\text{out}} - \dfrac{I_{T0}}{C\cdot d_0^2}\Delta d \end{cases} \tag{6}$$

Applying Laplace in system zero initial conditions, Eq. (6) results in transfer functions of the form

$$\frac{\Delta U_{\text{out}}}{\Delta U_{\text{in}}} = \frac{R_S\cdot d_0}{s^2(R_S\cdot L\cdot C) + L\cdot s + R_S} \tag{7}$$

$$\frac{\Delta U_{\text{out}}}{\Delta d} = \frac{R_S\cdot U_{\text{in}0}}{s^2(R_S\cdot L\cdot C) + L\cdot s + R_S} \tag{8}$$

Buck converter parameters considered in this chapter are $L = 56.5\ \mu\text{F},\ C = 166.7\ \mu\text{F},\ R_S = 2\ \Omega$, $d = 0.5,\ \ U_{\text{in}0} = 24\ \text{V},\ U_{\text{out}0} = 12\ \text{V}$. Simulation scheme for the buck converter with transfer functions, open loop is shown in **Figure 11**. Simulation results are presented in **Figure 12**. Utilizing a closed loop scheme and the same fuzzy controllers, like in the case of boost converter shown in **Figure 4**, closed-loop simulation results are obtained shown in **Figure 13**. For the buck converter control, a classical PI fuzzy controller has been designed with two inputs, the error between the output voltage and the voltage prescribed and integral of this error. Simulation scheme in this case is the one in **Figure 14**. The membership functions and control surface of this

http://dx.doi.org/10.5772/67992

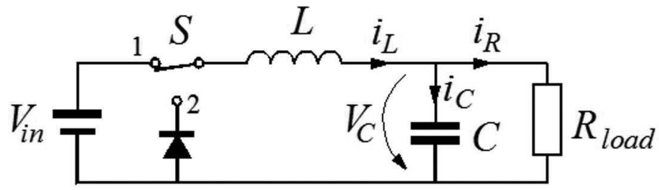

Figure 9. Principal scheme of buck converter.

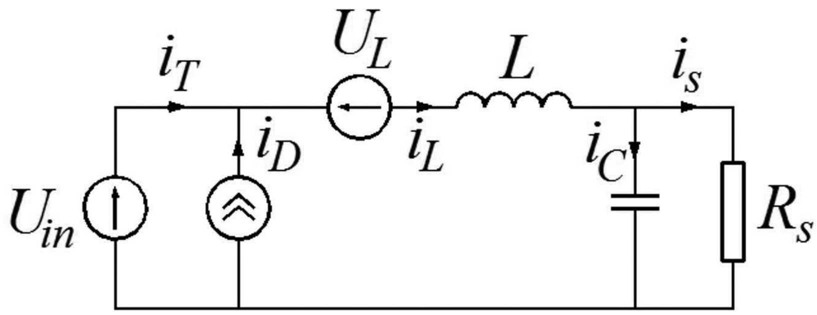

Figure 10. Equivalent scheme for continuous mode of buck converter.

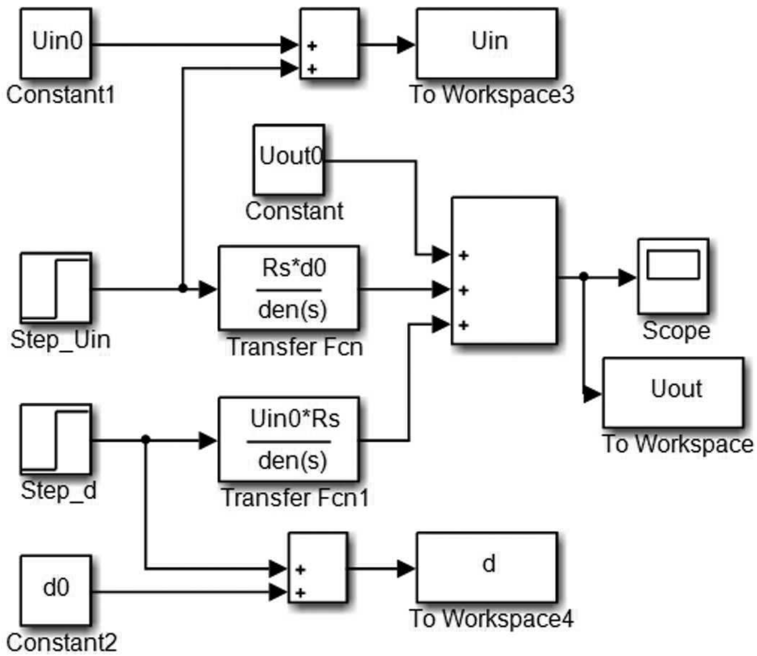

Figure 11. Open loop simulation scheme for buck converter.

controller are presented in **Figure 15**. The inference rules of fuzzy PI controller here are defined in table of this **Figure 16**. Buck converter behaviour with this control is shown in **Figure 17**. Note that the peak voltage obtained from step input is reduced to one third of the peak voltage obtained with the controller in the previous case (fuzzy controllers P and I are put in parallel), and the time to restore the prescribed value is also diminished.

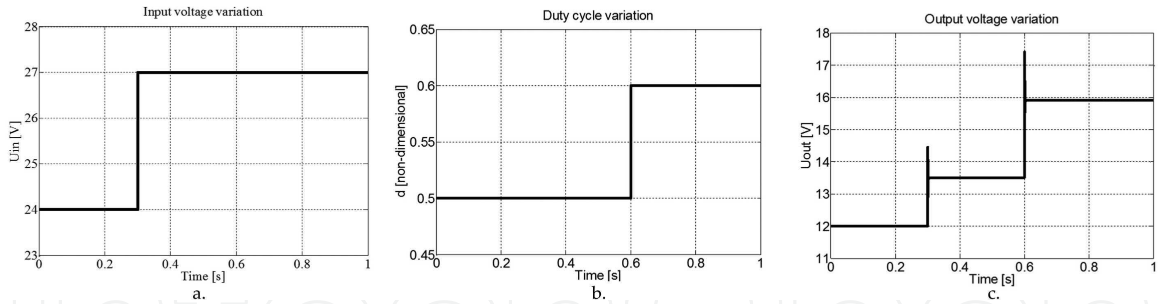

Figure 12. Open loop behaviour of buck converter: (a) input voltage variation; (b) duty cycle variation; (c) output voltage variation.

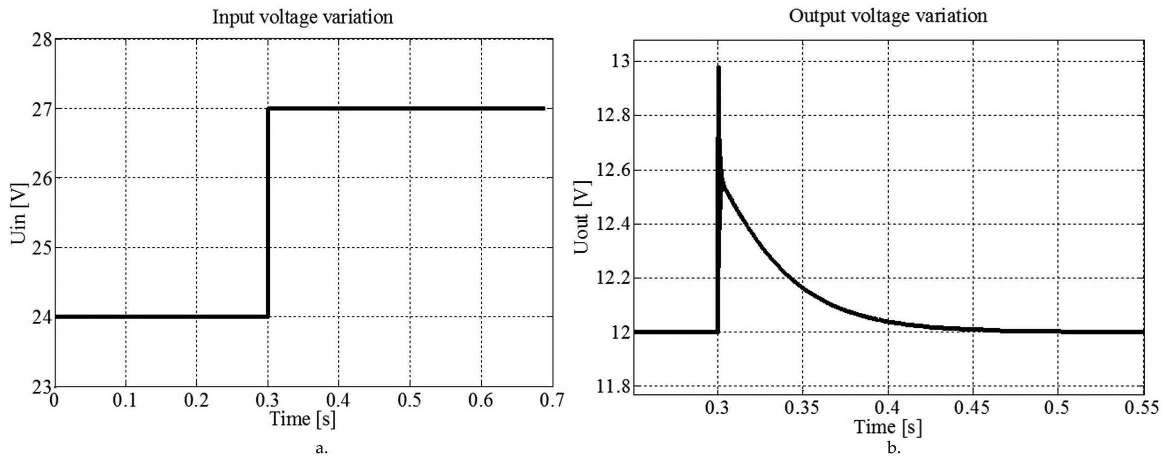

Figure 13. Closed loop behaviour of buck converter with two fuzzy controllers in parallel P+I: (a) input voltage variation; (b). output voltage variation.

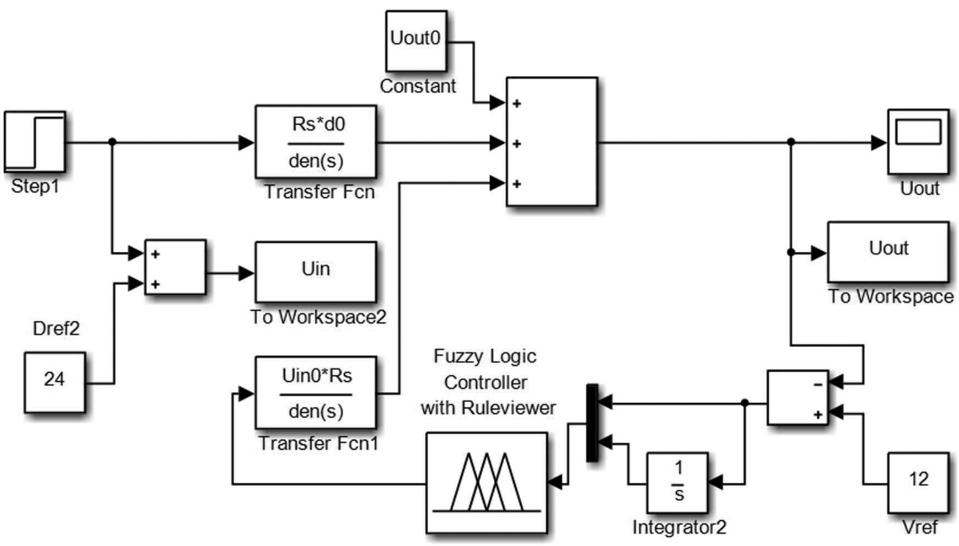

Figure 14. Closed loop simulation scheme for buck converter with one PI fuzzy controller with two inputs.

http://dx.doi.org/10.5772/67992

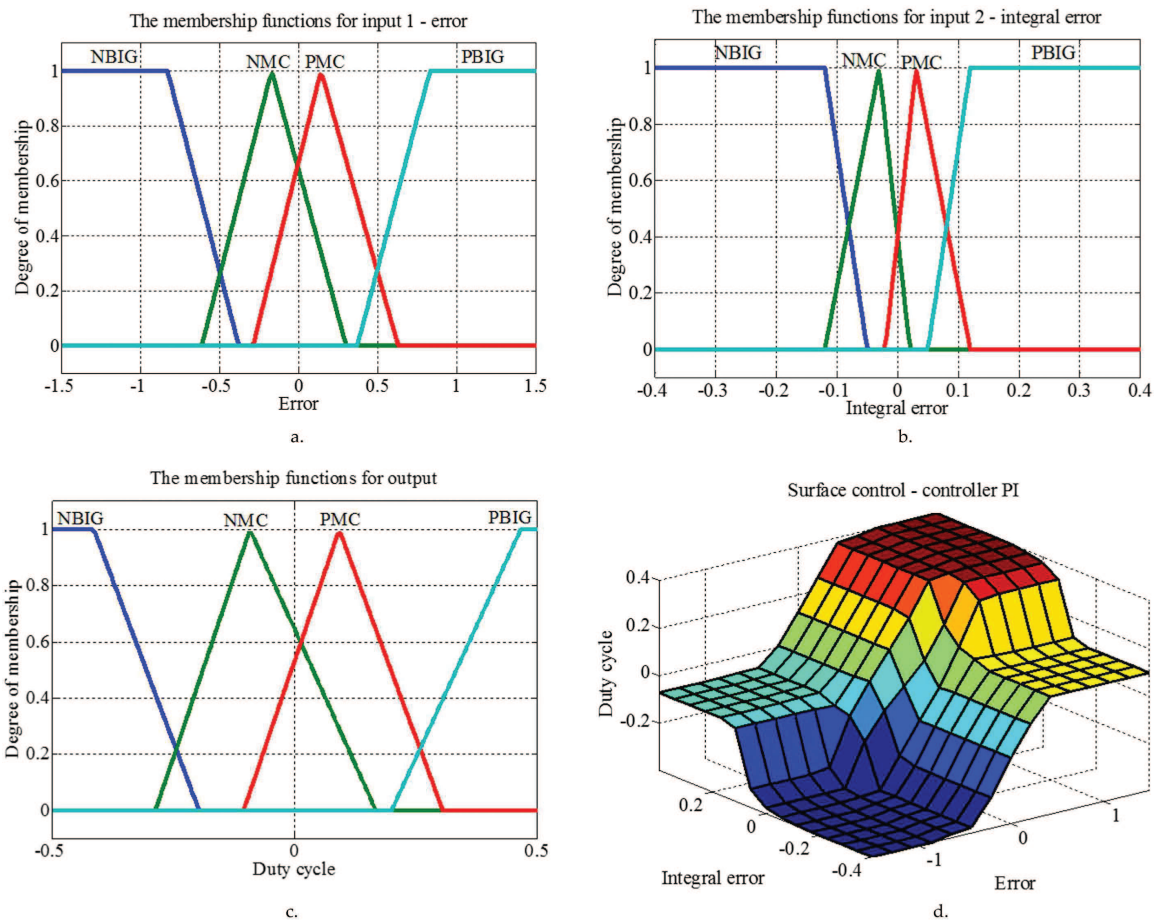

Figure 15. PI fuzzy controller with two inputs: (a) membership functions for error input; (b) membership functions for integral error input; (c) membership functions for output; (d) control surface.

		ERROR			
		NBIG	NMC	PMC	PBIG
ERROR INTEGRAL	NBIG	NBIG	NBIG	PMC	PMC
	NMC	NBIG	NBIG	PMC	PBIG
	PMC	NBIG	NMC	PBIG	PBIG
	PBIG	NMC	NMC	PBIG	PBIG

Figure 16. Inference rules for PI fuzzy controller with two inputs.

So, we can say that this second fuzzy PI controller with two inputs provides better behaviour, but at the expense of greater computation time, so microcontroller that is implemented should have better performance.

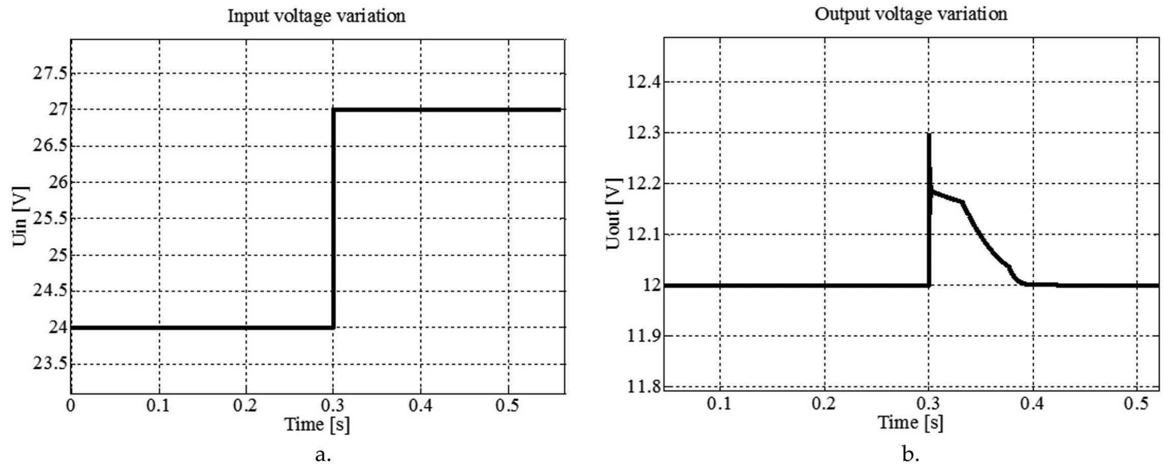

Figure 17. Closed loop behaviour of buck converter with PI fuzzy controller with two inputs: (a) input voltage variation; (b) output voltage variation.

4. Buck-boost converter

Principle scheme of the buck-boost converter is in **Figure 18**. This converter outputs a higher or a lower voltage than the input voltage but with inverse polarity, so it is known as controller-inverter. It also functions in two steps. In step 1, when the switch is in position 1, the diode is inversely polarized and the current flows from the source through the inductor and charges its electromagnetic field. In the second step, when the switch is in position 2, the energy stored in the inductor is released on the capacitor and the output load with inverse polarity of the voltage.

From the point of view of the average values, it was considered a voltage drop occurs on the switch. Also one considered the coil average voltage is equal with continuous output voltage. Following **Figure 19**, one can write the following relations: $i_S + i_C = i_D$, $i_D + i_T = i_L$, $U_L = U_{\text{in}} \cdot \frac{d}{d-1}$, $i_T(d-1) = i_D \cdot d$. It has considered among others stationary input-output characteristics of buck-boost converter. In addition, one can write the following equations:

$$U_{\text{in}} + U_T - U_L = -L\frac{di_L}{dt} \tag{9}$$

$$U_{\text{in}} = -L\frac{di_L}{dt} + R_S i_S \tag{10}$$

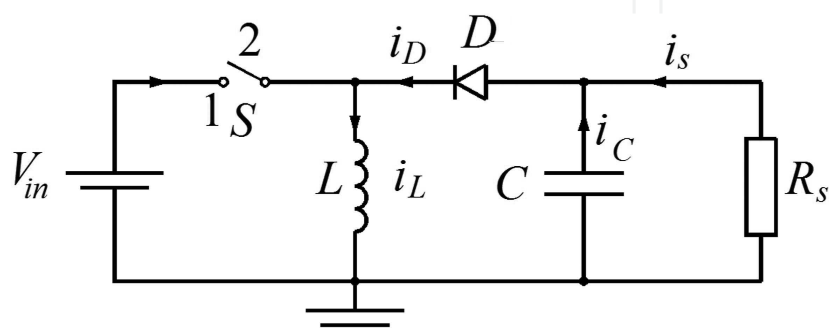

Figure 18. Principle scheme of buck-boost converter.

http://dx.doi.org/10.5772/67992

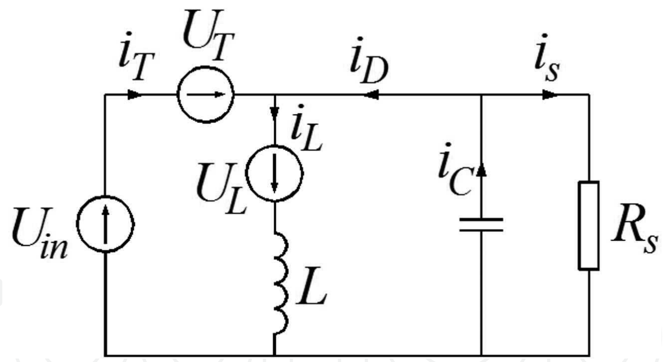

Figure 19. Equivalent scheme for continuous mode of buck-boost converter.

$$C\frac{dU_{\text{out}}}{dt} + \frac{U_{\text{out}}}{R_S} + i_T = i_L \tag{11}$$

After several transformations, we obtain:

$$U_{\text{out}} - U_{\text{in}}\frac{d}{d-1} = -L \cdot C\frac{d^2U_{\text{out}}}{dt^2} \cdot \frac{1}{d-1} + \frac{L}{R_S}\frac{dU_{\text{out}}}{dt} \cdot \frac{1}{d-1} \tag{12}$$

By linearization and applying Laplace transform in null initial conditions, transfer functions result as follows:

$$\frac{\Delta U_{\text{out}}(s)}{\Delta U_{\text{in}}(s)} = \frac{\frac{d_0}{d_0-1}}{-L \cdot C\frac{d_0}{d_0-1}s^2 - \frac{L}{R_S \cdot} \cdot \frac{d_0}{d_0-1}s + 1} \tag{13}$$

$$\frac{\Delta U_{\text{out}}(s)}{\Delta d(s)} = \frac{-U_{\text{in}0}\frac{1}{(d_0-1)^2}}{-L \cdot C\frac{d_0}{d_0-1}s^2 - \frac{L}{R_S \cdot} \cdot \frac{d_0}{d_0-1}s + 1} \tag{14}$$

Parameters used in the simulation buck-boost converter are: $L = 56.5\ \mu\text{F}$, $C = 166.7\ \mu\text{F}$, $R_S = 2\ \Omega$, $d = 0.5$, $U_{\text{in}0} = 15$ V, $U_{\text{out}0} = -15$ V. Scheme simulation for buck-boost converter in open circuit is similar to that for buck converter in **Figure 11**. Responses to step signals applied to both voltage input, and on the duty cycle are shown in **Figure 20**. Although for this converter two versions of fuzzy controllers were made, one version with two fuzzy controllers disposed in parallel, one for the proportional component and one for the integrative component, and a second version with a single fuzzy controller with two inputs (proportional and integrative) and one output (duty cycle variation). For the first variant, fuzzy controllers are shown in **Figures 21** and **22**. Buck-boost converter case has chosen five membership functions, one of which corresponds to the term linguistic ZERO (ZE in **Figures 21** and **22**), the other membership functions corresponding to the same linguistic terms as with previous fuzzy regulators. The inference rules in this case were the same for both controllers: If the input is NBIG, then output is NBIG; If the input is NMIC, then output is NMIC; If the input is ZE, then output is ZE; If the input is PMIC, then output is PMIC; If the input is PBIG, then output is PBIG.

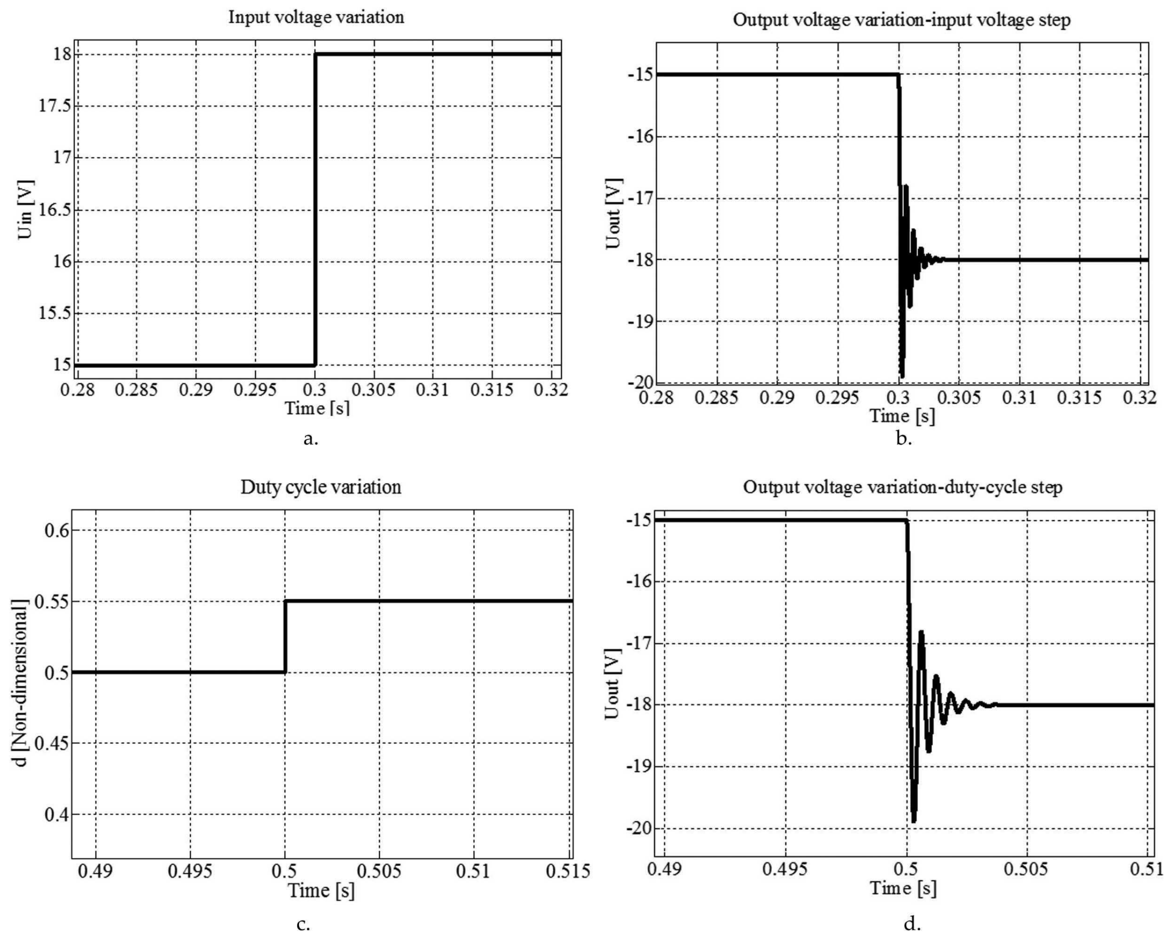

Figure 20. Buck-boost converter behaviour in open loop: (a) input voltage step; (b) output voltage at input voltage step; (c) duty cycle step; (d) output voltage at duty cycle step.

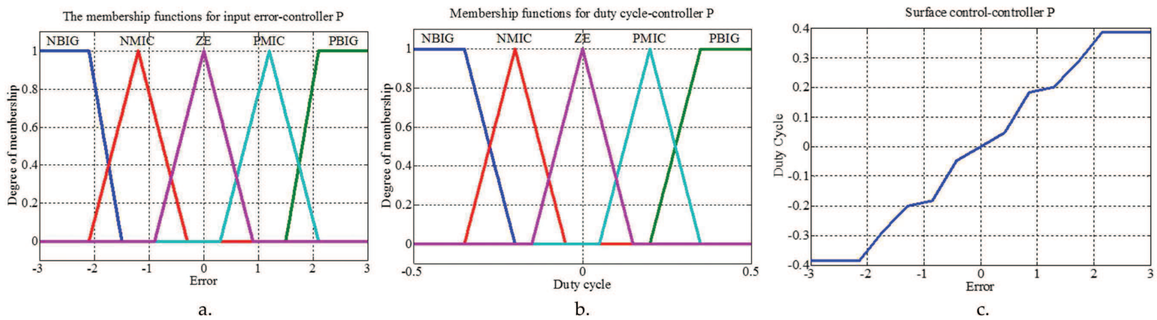

Figure 21. P fuzzy controller for buck-boost converter: (a) membership functions for input; (b) membership functions for output; (c) control surface.

Closed-loop simulation scheme for this case is similar to that for boost converter in **Figure 4** but with transfer functions and controllers shown in buck-boost converter. Buck-boost converter's response in a closed loop and step input are shown in **Figure 23**.

The behaviour of the converter for sinusoidal input voltage variation has been studied in this case which is shown in **Figure 24**.

http://dx.doi.org/10.5772/67992

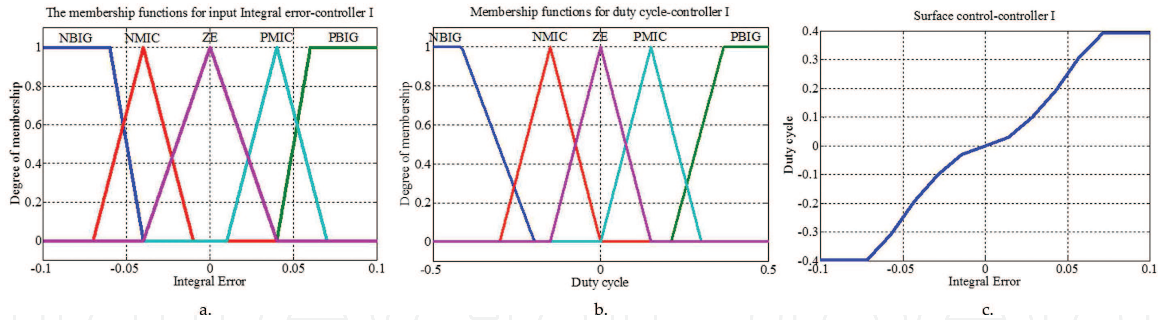

Figure 22. I fuzzy controller for buck-boost converter: (a) membership functions for input; (b) membership functions for output; (c) control surface.

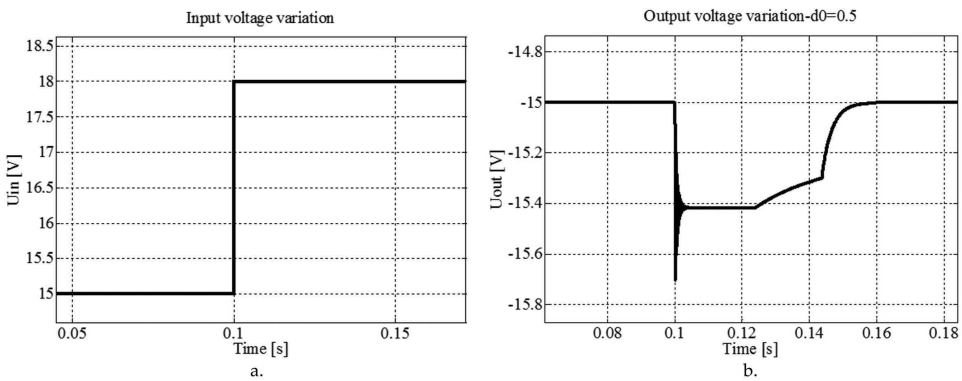

Figure 23. Closed loop behaviour of buck-boost converter with two fuzzy controllers in parallel (P+I): (a) input voltage variation; (b) output voltage variation.

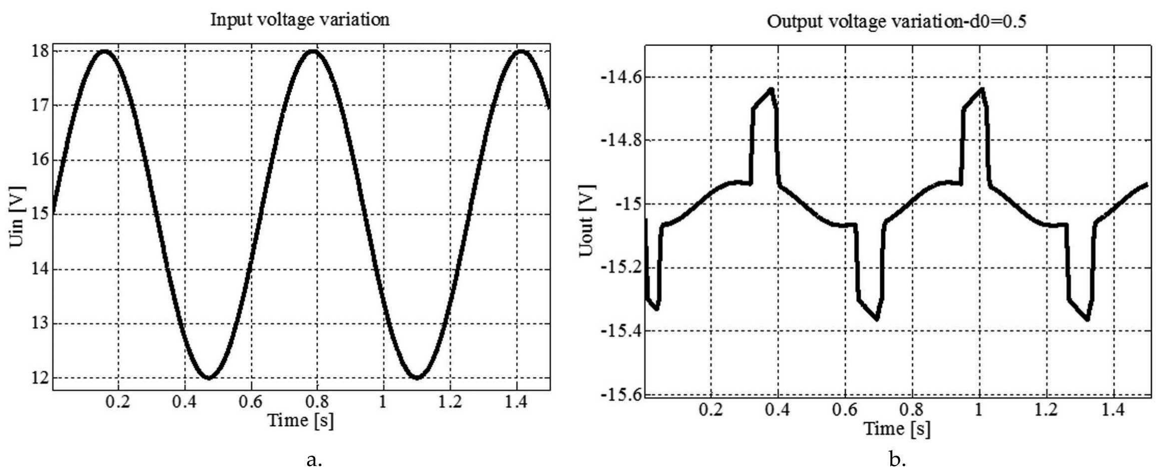

Figure 24. Closed loop behaviour of buck-boost converter with two fuzzy controllers in at sinusoidal input: (a) input voltage variation; (b) output voltage variation.

We notice here a better behaviour of fuzzy controller at step signal, the restore time to prescribed value is lower than the other controller presented converters but notice a worsened behaviour for sinusoidal signal response. At zero-crossing of the input signal, one obtained jumps in output voltage. The amplitude is not large, about 0.3 V, but these jumps means higher

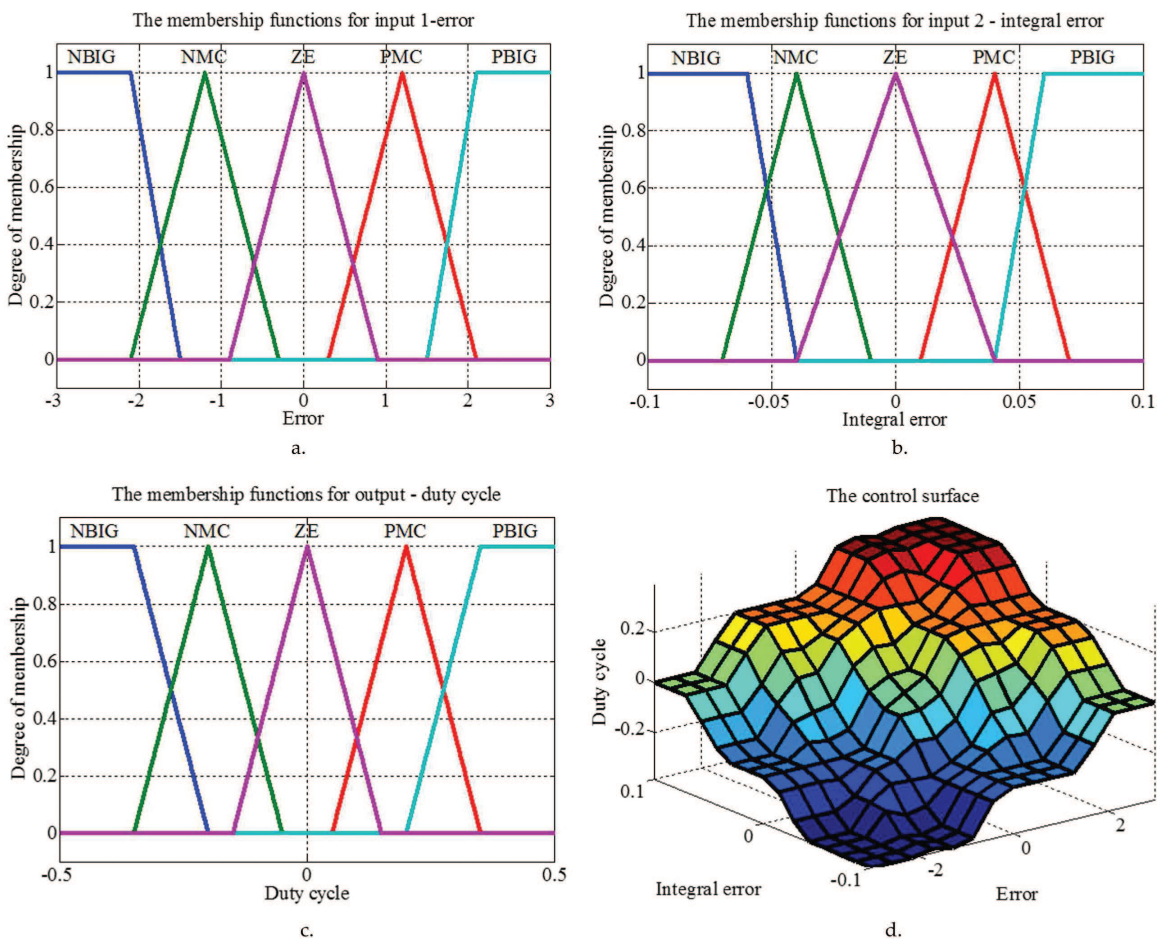

Figure 25. PI fuzzy controller with two inputs for buck-boost converter: (a) membership functions for proportional input; (b) membership functions for integral input; (c) membership functions for output; (d) control surface.

		ERROR				
		NBIG	NMC	ZE	PMC	PBIG
ERROR INTEGRAL	NBIG	NBIG	NBIG	NMC	NMC	ZE
	NMC	NBIG	NMC	NMC	ZE	PMC
	ZE	NMC	NMC	ZE	PMC	PMC
	PMC	NMC	ZE	PMC	PMC	PBIG
	PBIG	ZE	PMC	PMC	PBIG	PBIG

Figure 26. Inference rules for PI fuzzy controller.

harmonics induced on power bus and thus worsening power quality on board of the UAVs. A second version of fuzzy controller designed for buck-boost converter is that of a controller with two inputs and one output, with five membership functions on each input and the output. This fuzzy controller is shown in **Figure 25**. Inference rules for this fuzzy controller are presented in table in **Figure 26**.

One observes a good response at step input in this case; but at sinusoidal input, voltage peaks appear again at input zero crossing. That means again worse energy quality on board.

5. Conclusions

This paper presents some applications of the fuzzy control technique to DC-DC converters in usual configurations (boost, buck, buck-boost). For each converter, first averaged mathematical models are presented, obtained upon some equivalent schemes for continuous regime. Upon these averaged models, transfer functions for each converter are deduced. These transfer functions are applicable for the transitory regimes in the small perturbation hypothesis. One has to take into account that the averaged models and transfer functions are available for the continuous conduction regime for each converter. In order to obtain the continuous conduction regime, each of the studied converters needs a big enough switching frequency. This frequency does not appear explicitly in the transfer functions, but is determined by the circuit components.

Fuzzy controllers developed here for the studied converters are less usual. First, for the boost and buck converters, one used fuzzy controllers with four membership functions two on each input and output. In order to diminish the calculus volume for each functioning step as much as possible, one used triangular membership functions at the middle of the interval and trapezoidal membership functions at extremities. Although, one followed to reduce the number of membership functions.

For a more stable behaviour of the converters, one tried to reduce the control surface slope around the origin and to keep a bigger slope far from the origin, in order to accelerate converter return to the desired functioning point. By a convenient choose of the membership functions, one could reach this purpose in conditions of a small number of membership functions, as one can see in **Figures 5c**, **6c** and less in **Figure 15d**.

To reduce further the calculus volume at each functioning step and to simplify inference rules definition, one tested the possibility to decompose a PI fuzzy controller with two inputs in two simpler fuzzy controllers, each of them with one input. These new fuzzy controllers are disposed in parallel and one has as input the error between the real output voltage and the desired output voltage, and the other has as input the integral of this error. In this way, one can reduce the inference rules from $n \times n$ to $2 \times n$ where n is the number of the membership functions. Fuzzy controllers defined for the boost converter were used successfully to control the buck converter.

For buck converter, one designed a classical PI fuzzy controller with two inputs and one output, with four membership functions, two on each input an on the output (see **Figure 15**). Performances obtained with this controller are improved. The peaks on the output voltage are reduced, and time to return to the prescribed voltage is also reduced (see **Figure 17**). In **Figure 17**, one observes response slope changes when the controller passes from a control interval to another and the return acceleration when the integrative component reaches the limit of membership function PMC. One observes further response of slope diminishing when the error decreases and smooth approach of the real output voltage to the prescribed one.

For the buck-boost converter, one tested classical fuzzy converters with odd number of membership functions on each input (one of them corresponding to the linguistic term ZERO). One aimed to obtain for this controller a small slope of the control surface near the origin and a bigger slope far from it. Designed controllers can be seen in **Figures 21**, **22** and **25**. Buck-boost converter behaviour is good when step input is used, as one can see in **Figures 23** and **27**. But when sinusoidal input is used, problems appear. In **Figures 24** and **27** one can see the output voltage peaks when the input passes through zero. That means worse quality of energy on board.

As an important conclusion, one can say that control with fuzzy technique offers a special flexibility to the controller design. One can reach very good performances even for simplified configurations of the controller. Possibility to obtain a convenient control surface for each

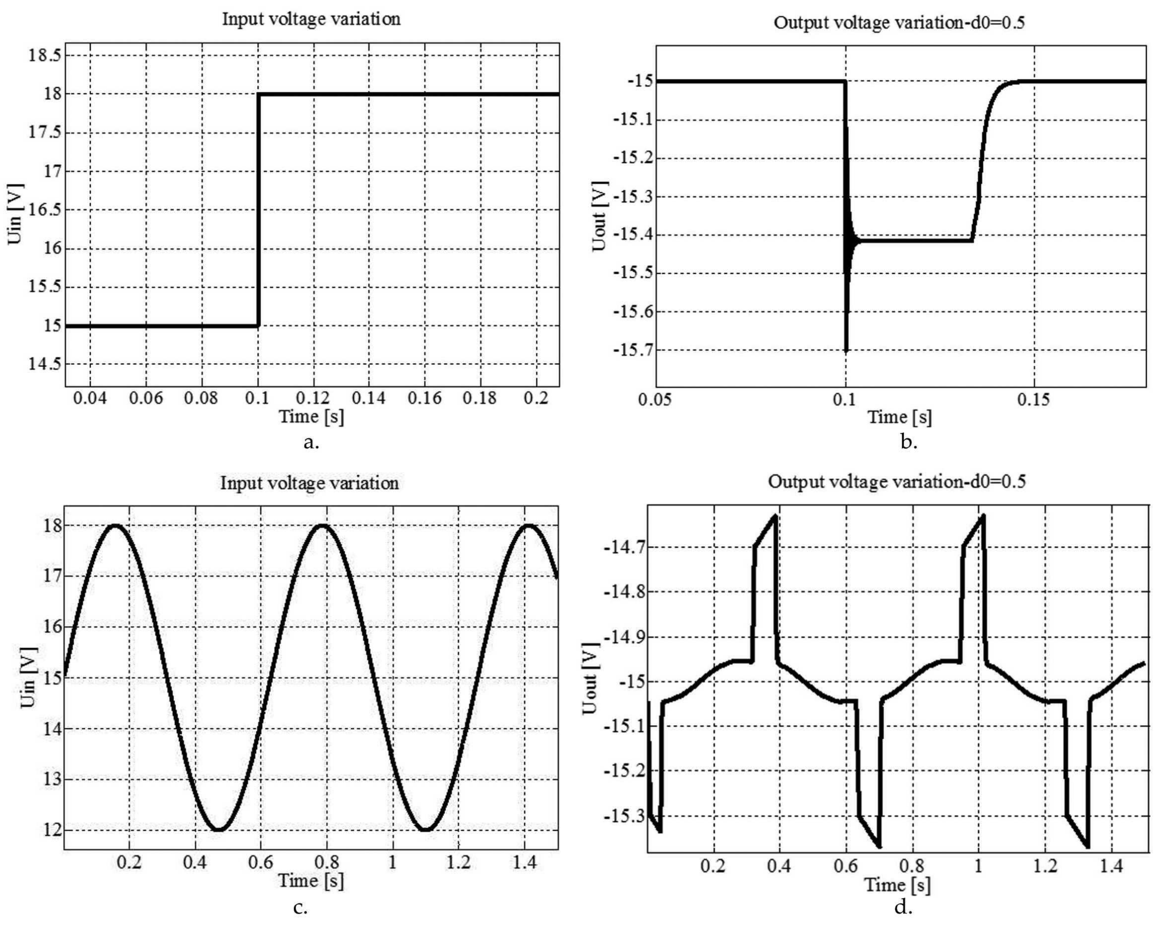

Figure 27. Buck-boost converter behaviour with PI fuzzy controller: (a) voltage step input; (b) response to step input; (c) sinusoidal voltage input; (d) response to sinusoidal input.

application is an advantage that cannot be reached with other control techniques. Although, in some cases, design of a good fuzzy controller needs some experience and testing of many variants, in order to select the better one. Simplistic definition of the membership functions and inference rules can lead either to inconvenient control surfaces or to linear ones. In the second case, the fuzzy controller could be replaced very well with a classical P or PI controller, with same performances.

Author details

Dinca Liviu* and Corcau Jenica Ileana

*Address all correspondence to: ldinca@elth.ucv.ro

Department of Electrical, Energetic and Aerospace Engineering, Faculty of Electrical Engineering, University of Craiova, Craiova, Romania

References

[1] P. O'Neil. Boeing High Altitude Long Endurance (HALE) UAS, available at https://higherlogicdownload.s3.amazonaws.com/AUVSI/656942e4-4448-41c3-877d-0c5f3ea40e63/UploadedImages/KnowledgeVault/HALE.pdf

[2] N. Owano. Titan Aerospace readies solar-powered, long-endurance UAVs; 22 August 2013. www.boeing.com/defense/phantom-eye [Internet].

[3] H. Ross. www.solarimpulse.com [Internet]; May 2009.

[4] F. Misoc. A comparative study of dc–dc converters' effects on the output characteristics of direct ethanol fuel cells and NiCd batteries [dissertation]. Thesis of Dissertation Kansas State University, Manhattan, Kansas; 2007.

[5] M. H. Rashid. Power Electronics Circuits, Devices, and Applications. 3rd edition. University of West Florida, Pearson Prentice Hall; 2003.

[6] R. W. Erickson, D. Maksimovic. Fundamentals of Power Electronics. 2nd edition. 912 p. Kluwer Academic Publishers 2001, Sixth Printing 2004, DOI: ISBN 0-7923-7270-0.

[7] G. Feng, W. Zhang, Y.-F. Liu. An Adaptive Current Mode Fuzzy Logic Controller for Dc-to-Dc Converters. Eighteenth Annual IEEE Applied Power Electronics Conference and Exposition; Miami Beach, Florida, 2003; pp. 983–989.

[8] P. Mattavelli, L. Rossetto, G. Spiazzi, P. Tenti. General-Purpose Fuzzy Controller for Dc/Dc Converters. In: Applied Power Electronics Conference, Dallas, Texas 1995.

[9] A. G. Perry, G. Feng, Y.-F. Liu, P.C. Sen. A New Design Method for PI-like Fuzzy Logic Controllers for DC-to-DC Converters. In: 35th Annual IEEE Power Electronics Specialists Conference; 2004; pp. 3751–3757.

[10] A. Gad, M. Farooq. Application of Fuzzy Logic in Engineering Problems. Proceedings of the 27th annual conference of the IEEE Industrial Electronics Society (IECON 01), Denver, CO, 29 November-2 December 2001; p. 2044–2049.

[11] B. Johansson. DC-DC converters-dynamic model design and experimental verification [thesis]. Lund University: Doctoral Dissertation in Industrial Automation Department of Industrial Electrical Engineering and Automation; 2004.

[12] M. Salimi, A. Zakipour. Direct voltage regulation of DC-DC buck converter in a wide range of operation using adaptive input-output linearization. In: IEEE Transactions on Electrical and Electronic Engineering, January 2015; pp. 85–91. DOI: ISSN 1931–4973.

[13] J. Chen, D. Maksimovic, R. Erickson. Buck-boost PWM converters having two independently controlled switches. In: Proc. IEEE Power Electronics Specialists Conference; Vancouver Canada, June 17–21, 2001; pp. 736–741.

[14] L. Guo. Design and implementation of digital controllers for buck and boost converters using linear and nonlinear control methods [dissertation]. Auburn University, Alabama; 2006.

[15] H. Fadali. Fuel cell distributed generation, power conditioning, control and energy management [dissertation]. Master of Applied Science in Electrical and Computer Engineering, Ontario, Canada; 2008.

[16] P. Hemachander, A. D. VimalRaj, M. Sudhakaran. Analysis design and implementation f soft single switched boost converter. In: International Journal of Computer Applications; 26(11), July 2011; pp. 38–46.

[17] P. S. Priambodo, D. Sukoco, W. Purnomo, H. Sudibyo, D. Hartanto., Electric Energy Management and Engineering in Solar Cell System. Chapter 12 in book “Solar cells – Research and Application Perspectives” editor Arturo Morales-Acevedo, published by INTECH on 6th March 2013; pp. 327–351.